Supporting Information

Aggregation-Induced Emission Characteristics of *o*-Carborane-Functionalized Fluorene and Its Heteroanalogs: The Influence of Heteroatoms on Photoluminescence

Xueyan Wu,[a] Jixi Guo,[*a] Yan LV,[a] Dianzeng Jia,[*a] Jianzhang Zhao,[a,b] Huici Shan,[a] Xiaoping Jin,[a] Yongdong Ma[a]

[a] Key Laboratory of Energy Materials Chemistry, Ministry of Education; Key Laboratory of Advanced Functional Materials, Autonomous Region; Institute of Applied Chemistry, Xinjiang University, Urumqi 830046, P. R. China. Email: jxguo1012@163.com; jdz@xju.edu.cn.

[b] State Key Laboratory of Fine Chemicals, Dalian University of Technology, 2 Linggong Road, Dalian 116024, P. R. China.

Table of Contents

1. UV–Vis absorption and fluorescence emission spectra of the compounds

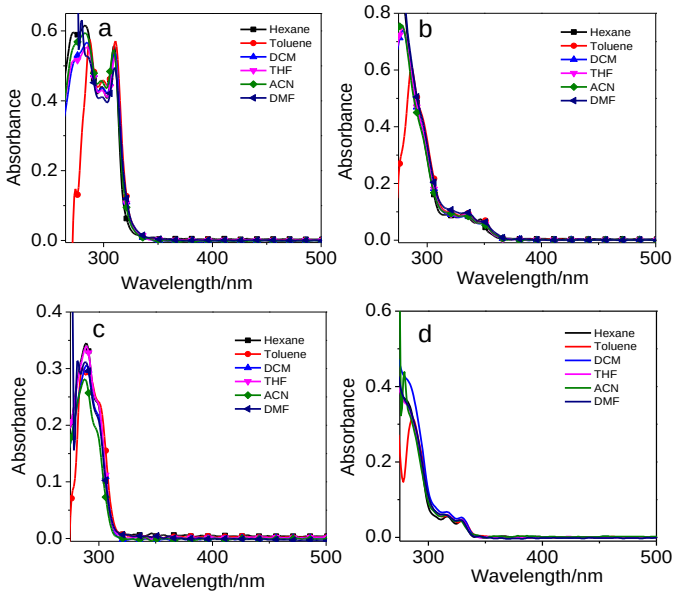

Figure S1. UV-Vis absorption spectra of (a) **CDC**, (b) **CDN** (c) **CDO** and (d) **CDS** in various solvents, c = 1.0 × 10^{-5} M, 20 ^{o}C.

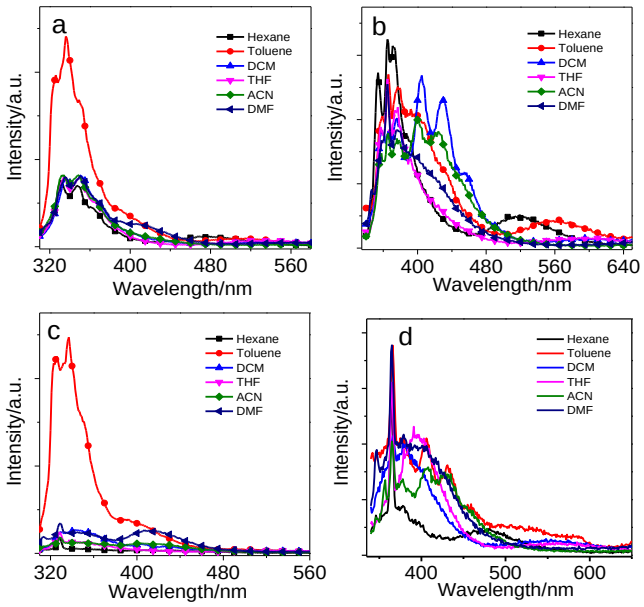

Figure S2. The emission spectra of (a) **CDC**, (b) **CDN** (c) **CDO** and (d) **CDS** in various solvents, λ_{ex} = 300 nm for **CDC** and **CDO**, λ_{ex} = 330 nm for **CDN** and **CDS**, c = 1.0 × 10^{-5} M, 20 ^{o}C.

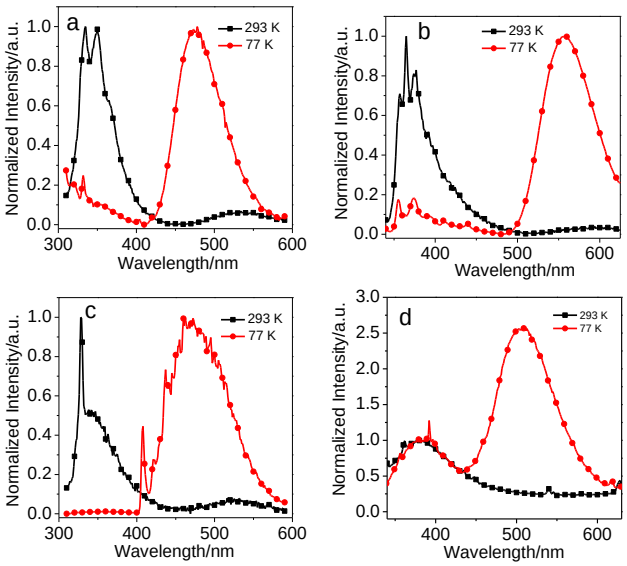

Figure S3. The PL spectra of (a) **CDC**, (b) **CDN** (c) **CDO** and (d) **CDS** in 2-MeTHF at r.t. (black line) and 77 K (red line), λ_{ex} = 300 nm for **CDC** and **CDO**, λ_{ex} = 330 nm for **CDN** and **CDS**, c = 2.0 $\times 10^{-5}$ M.

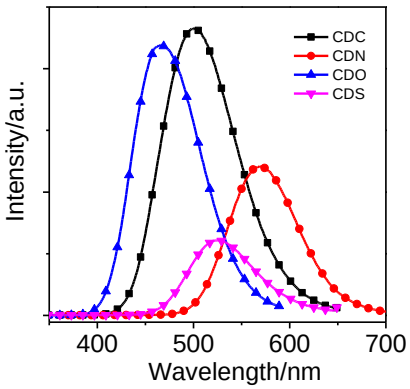

Figure S4. The emission spectra of **CDC**, **CDN**, **CDO** and **CDS** in the solid state, λ_{ex} = 300 nm for **CDC** and **CDO**, λ_{ex} = 330 nm for **CDN** and **CDS**, 20 ^{o}C.

2. Time-resolved Florescence Measurements

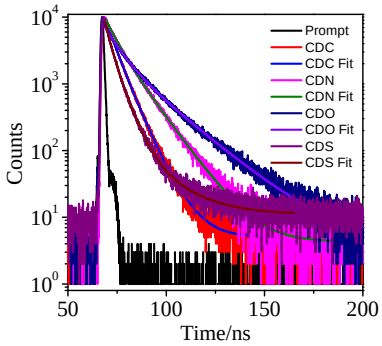

Figure S5. Emission decay profiles of **CDC**, **CDN**, **CDO** and **CDS** in the mixture of THF and water, f_w = 99%, c = 5.0 × 10^{-5} M, λ_{ex} = 340 nm, 20 °C.

3. Crystal Packing from X-ray Crystallography of the compounds

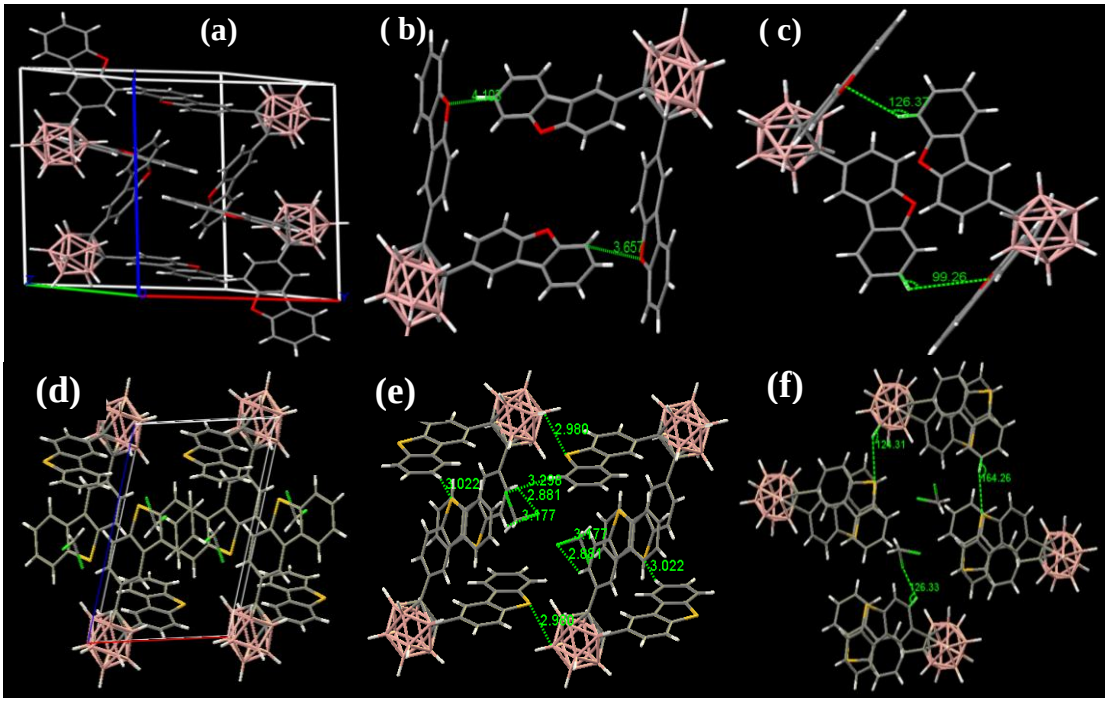

Figure S6. The unit cells of (a) **CDO** and (d) **CDS**, (b) C–H ··O and (e) B–H ··S, C–H ··Cl lengths, (c) C–H ··O and (f) B–H ··S, C–H ··S, C–H ··Cl angles.

Table S1. Crystal data and structure refinement for **CDO** and **CDS**.

Compounds	**CDO**	**CDS**
Empirical formula	$C_{26}H_{24}B_{10}O_2$	$C_{26}H_{24}B_{10}S_2{\cdot}CH_2Cl_2$
CCDC	1838965	1843555
Formula weight	476.55	593.60
Temperature	296 K	173 K
Wavelength	0.71073 Å	0.71073 Å
Crystal system	Monoclinic	Triclinic
Space group	$P2_1/c$	P-1
Unit cell dimensions	a = 14.0788(12) Å α = 90 Å. b = 11.9888(11) Å β = 95.346(2) Å. c = 15.4045(13) Å γ = 90 Å.	a = 10.3775(5) Å α = 74.141(1) Å. b = 2.6725(6) Å β = 69.041(1) Å. c = 12.9325(6) Å γ = 67.234(1) Å.
Volume	2588.8(4) $Å^3$	1446.41(12) $Å^3$
Z	4	2
Calculated density, mg/m^3	1.223	1.363
Absorption coefficient, mm^{-1}	0.069	0.389
F(000)	984.0	608.0
Crystal size, mm^3	0.3 ×0.25 ×0.2	0.2 ×0.17 ×0.13
Theta range for data collection	4.312 to 55.228 °	2.385 to 25.500 °
Index ranges	$-17 \le h \le 18, -15 \le k \le 15, -19 \le l \le 20$	$-12 \le h \le 12, -15 \le k \le 15, -15 \le l \le 15$
Reflections collected	21015	24462
Independent reflections	5992 [R_{int} = 0.0269, R_{sigma}= 0.0271]	5344 [R_{int} = 0.0372, R_{sigma}= 0.281]
Data / restraints / parameters	5992 / 0 / 343	5344 / 0 / 407
Goodness-of-fit on F^2	1.028	1.033
Final R indices [I>2sigma(I)]	R_1 = 0.0467, wR_2 = 0.1372	R_1 = 0.0603, wR_2 = 0.1591
R indices (all data)	R_1 = 0.0805, wR_2 = 0.1624	R_1 = 0.0645, wR_2 = 0.1632
Largest diff. peak and hole e.$Å^{-3}$	0.188 and -0.198	0.942 and -1.631

Table S2. Selected bond length [Å] and torsion angles [°] for **CDO** and **CDS**.

	Bond lengths [Å]		Bond angles[°]		Torsion angles[°]	
CDO	C(1)-C(2)	1.727(2)	C(3)-C(1)-C(2)	117.20(12)	C(3)-C(1)-C(2)-C(15)	-3.40(3)
	C(6)-O(1)	1.384(2)	C(15)-C(2)-C(1)	119.10(12)	C(1)-C(2)-C(15)-C(16)	89.9(3)
	C(7)-O(1)	1.390(2)	C(6)-O(1)-C(7)	105.22(14)	C(1)-C(2)-C(15)-C(26)	-97.0(2)
	C(18)-O(2)	1.3803(18)	C(18)-O(2)-C(19)	105.18(12)		
	C(19)-O(2)	1.386(2)				
	C(1)-C(3)	1.504(2)				
	C(2)-C(15)	1.4972(19)				
CDS	C(13)-C(14)	1.743(3)	C(11)-C(13)-C(14)	120.16(18)	C(11)-C(13)-C(14)-C(15)	-1.3(3)
	C(1)-S(1)	1.744(3)	C(15)-C(14)-C(13)	119.68(18)	C(13)-C(14)-C(15)-C(20)	75.9(3)
	C(8)-S(1)	1.745(2)	C(1)-S(1)-C(8)	91.29(12)	C(13)-C(14)-C(15)-C(16)	-108.4(2)
	C(18)-S(2)	1.743(3)	C(18)-S(2)-C(22)	91.19(13)		
	C(22)-S(2)	1.749(3)				
	C(11)-C(13)	1.501(3)				
	C(14)-C(15)	1.501(3)				

4. Electrochemical (CV) studies of the compounds

Electrochemical methods cyclic voltammetry (CV) was performed using a three-electrode cell linked to a model CHI760E electrochemical workstation (CH Instruments, Shanghai). The solution was purged with N_2 before measurement. A three-electrode cell system was used. including an $Ag/AgNO_3$ couple as the reference electrode. $c_{[Ag^+]}$ = 0.10 M, A platinum wire as a counter electrode and a modified glassy carbon electrode as a working electrode. Before each measurement, the working electrode (WE) was polished on a felt pad with 0.05 μm alumina (Tianjin Aida, Ltd.), wash with DI water. The potential values were calibrated with respect to the F_C/F_C^+ (F_C = Ferrocene) redox couple. Freshly distilled, degassed acetonitrile was used as the solvent, with 0.1 M Bu_4NPF_6 as the supporting electrolyte.

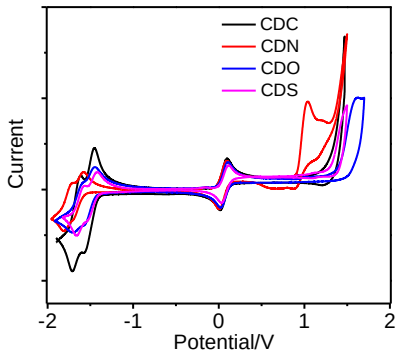

Figure S7. Cyclic voltammogram of **CDC**, **CDN**, **CDO** and **CDS**, c = 1.0 × 10^{-3} M. In the deaerated acetonitrile solution containing the compounds, 0.10 M Bu_4NPF_6 as supporting electrode, $Ag/AgNO_3$ as reference electrode, Scan rates: 100 mV/s. For all compounds Ferrocene (Fc) (c = 1.0 × 10^{-3} M) was used as internal reference, 20 ^oC.

5. DFT calculations

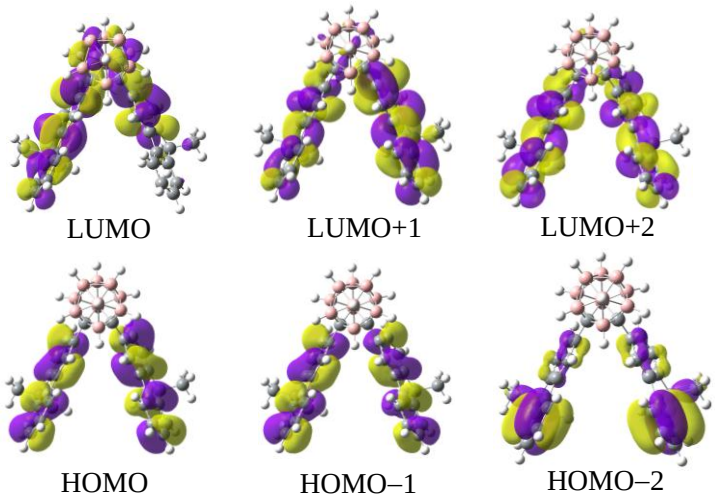

Figure S8. The theoretical calculated ground-state frontier orbitals contributions of **CDC** in gas sate using B3LYP/6-31G (d, p) level by Gaussian 09.

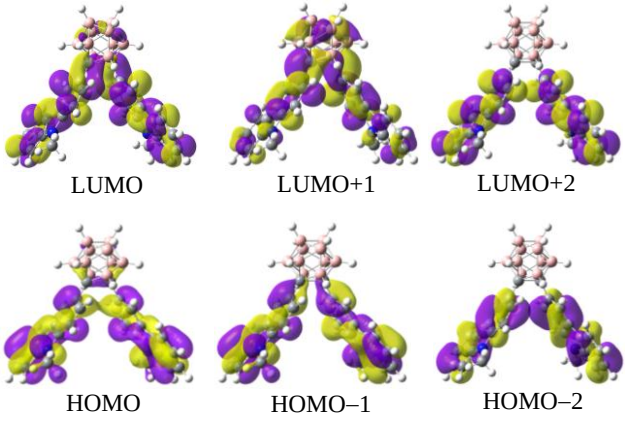

Figure S9. The theoretical calculated ground-state frontier orbitals contributions of **CDN** in gas sate using B3LYP/6-31G (d, p) level by Gaussian 09.

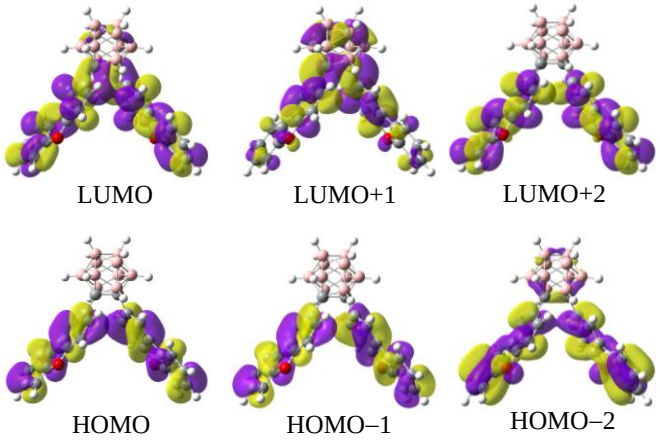

Figure S10. The theoretical calculated ground-state frontier orbitals contributions of **CDO** in gas sate using B3LYP/6-31G (d, p) level by Gaussian 09.

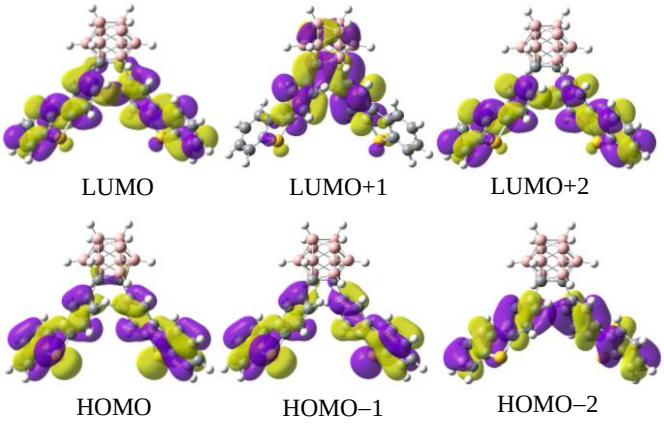

Figure S11. The theoretical calculated ground-state frontier orbitals contributions of **CDS** in gas sate using B3LYP/6-31G (d, p) level by Gaussian 09.

Table S3. Selected parameters for the UV-Vis absorption and Singlet state (Fluorescence) energy of the compounds. Electronic excitation energies (eV), oscillator strengths (*f*), and configurations of the low-lying excited states of **CDC** were calculated using TDDFT//B3LYP/6-31G(d, p), based on the optimized ground state geometries.

Comp	Electronic transition[a]		TDDFT/B3LYP/6-31G(d,p)		
			Excitation energy	f^b	Composition[c]
CDC	UV-Vis	$S_0 \rightarrow S_1$	4.23 eV (293 nm)	0.0323	H→L
		$S_0 \rightarrow S_2$	4.48 eV (277 nm)	0.1267	H–1→L+1
	Fluorescence	$S_0 \rightarrow S_1$	2.46 eV (504 nm)	0.0531	H→L
CDN	UV-Vis	$S_0 \rightarrow S_1$	3.94 eV (315 nm)	0.0282	H→L
		$S_0 \rightarrow S_2$	4.40 eV (282 nm)	0.3456	H–1→L
	Fluorescence	$S_0 \rightarrow S_1$	2.17 eV (572 nm)	0.1540	H→L
CDO	UV-Vis	$S_0 \rightarrow S_1$	4.33 eV (286 nm)	0.0779	H→L
		$S_0 \rightarrow S_2$	4.71 eV (263 nm)	0.1626	H→L+1
	Fluorescence	$S_0 \rightarrow S_1$	2.56 eV (485 nm)	0.2490	H→L
CDS	UV-Vis	$S_0 \rightarrow S_1$	4.09 eV (303 nm)	0.0137	H→L
		$S_0 \rightarrow S_2$	4.52 eV (274 nm)	0.1978	H→L+1
	Fluorescence	$S_0 \rightarrow S_1$	2.38 eV (520 nm)	0.1764	H→L

[a] Only selected excited states were considered. Numbers in parentheses are the excitation energy in wavelength. [b] Oscillator strength. [c] H stands for the HOMO and L stands for the LUMO. Only the main configurations are presented. [d] Coefficient of the wave function for each excitation. CI coefficients are given in absolute values.

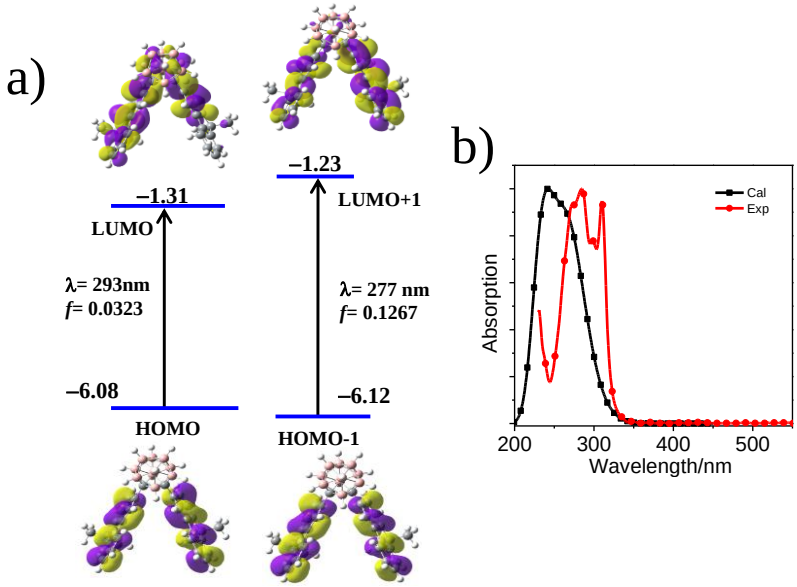

Figure S12. Frontier molecular orbitals for (a) **CDC** and (b) Simulated absorption spectra of **CDC** in ground state (S_0) optimized geometries in gas state and the lowest-energy electronic transition from TD-DFT calculation at the B3LYP/6-31G (d, p) level by Gaussian 09.

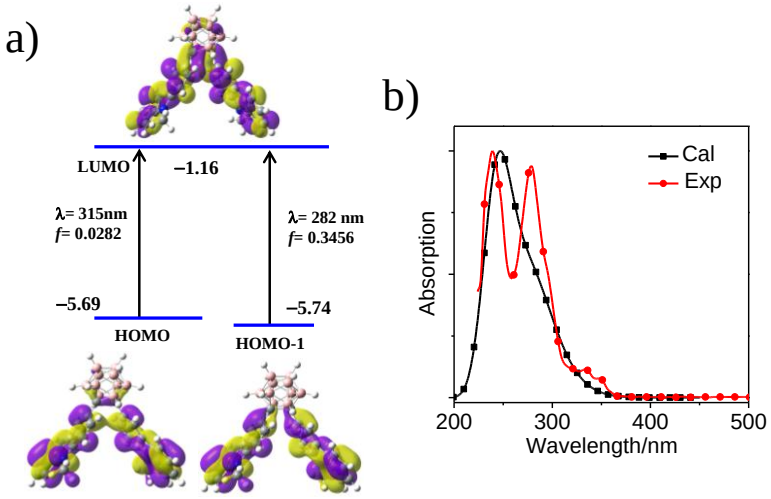

Figure S13. Frontier molecular orbitals for (a) **CDN** and (b) Simulated absorption spectra of **CDN** in ground state (S_0) optimized geometries in gas state and the lowest-energy electronic transition from TD-DFT calculation at the B3LYP/6-31G (d, p) level by Gaussian 09.

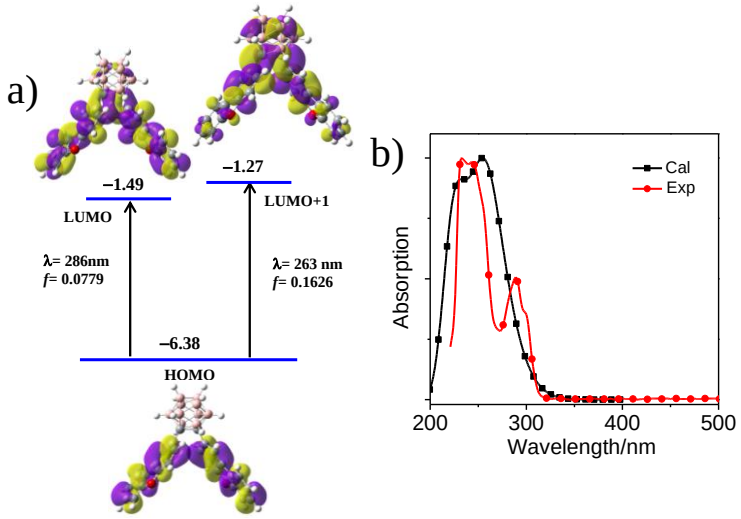

Figure S14. Frontier molecular orbitals for (a) **CDO** and (b) Simulated absorption spectra of **CDO** in ground state (S_0) optimized geometries in gas state and the lowest-energy electronic transition from TD-DFT calculation at the B3LYP/6-31G (d, p) level by Gaussian 09.

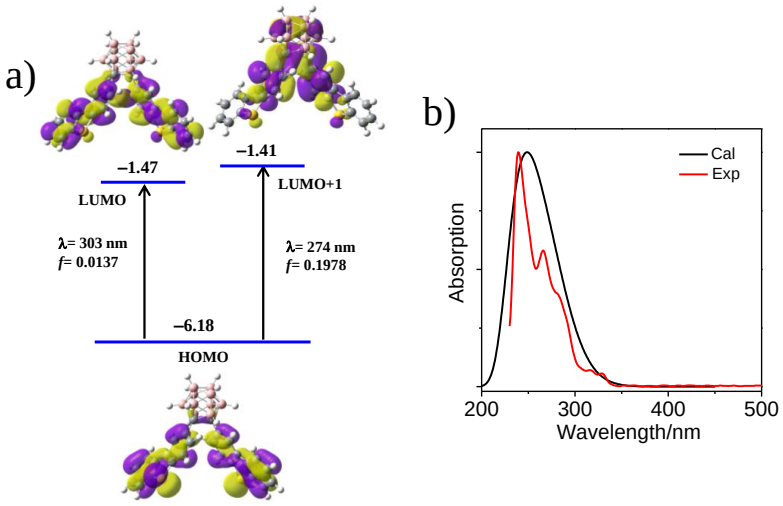

Figure S15. Frontier molecular orbitals for (a) **CDS** and (b) Simulated absorption spectra of **CDS** in ground state (S_0) optimized geometries in gas state and the lowest-energy electronic transition from TD-DFT calculation at the B3LYP/6-31G (d, p) level by Gaussian 09.

Table S4. The ground (μ_G) and excited (μ_E at the Franck−Condon geometry) dipole moments calculated with (TD-) DFT (B3LYP/6−31G (d, p)).

Compound	μ_G (Debye)	μ_E (Debye)	$\Delta\mu$ ($\mu_E - \mu_G$) (Debye)
CDC	8.05	22.17	14.12
CDN	10.16	21.93	11.77
CDO	6.56	21.74	15.81
CDS	6.06	19.27	13.21

6. NMR Spectra analysis of all target compounds

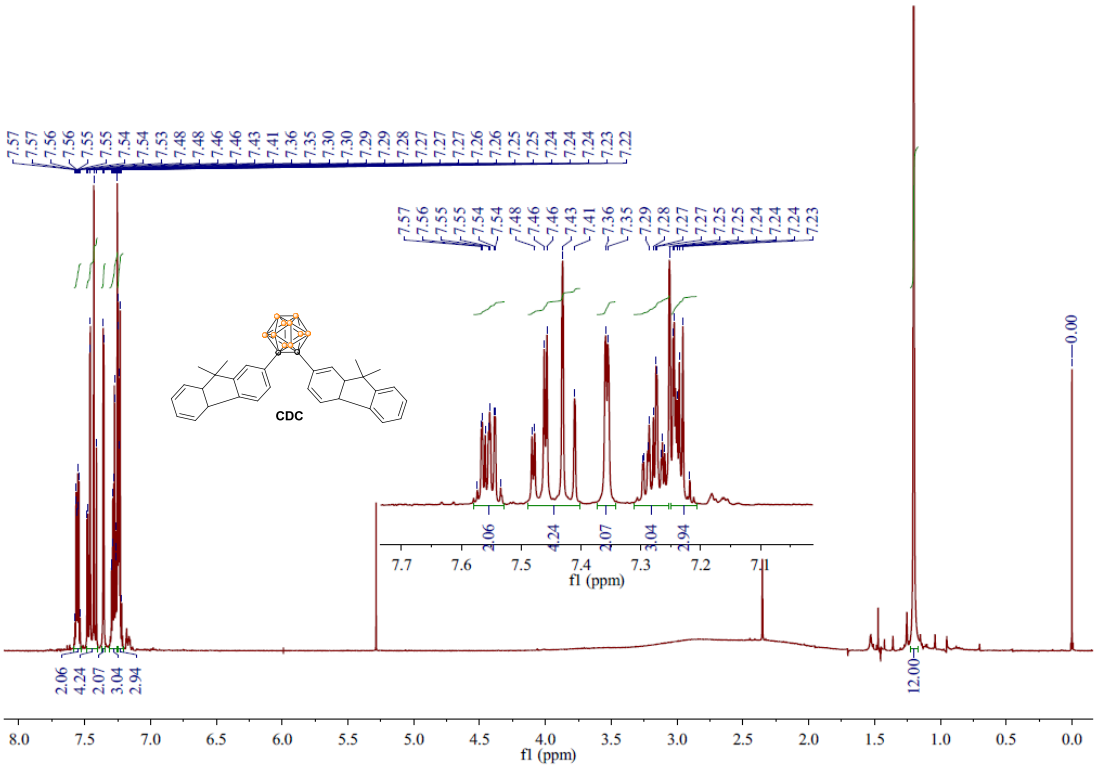

Figure S16. ^{1}H NMR spectroscopies of **CDC** in $CDCl_3$.

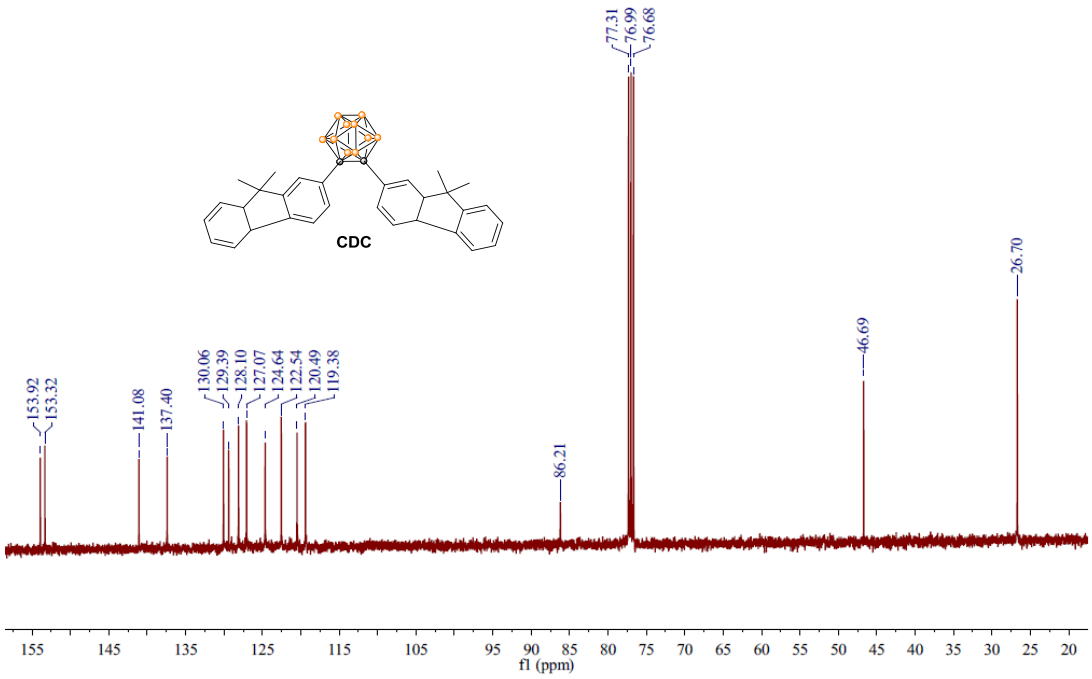

Figure S17. ^{13}C NMR spectroscopies of **CDC** in $CDCl_3$.

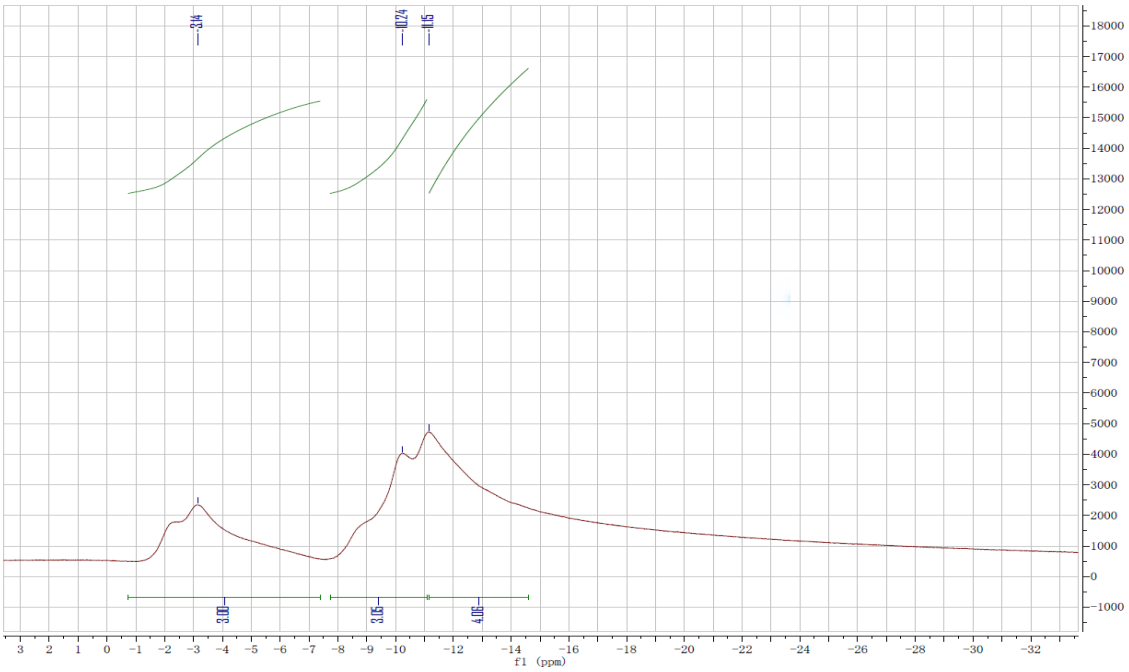

Figure S18. ^{11}B NMR spectroscopies of **CDC** in $CDCl_3$.

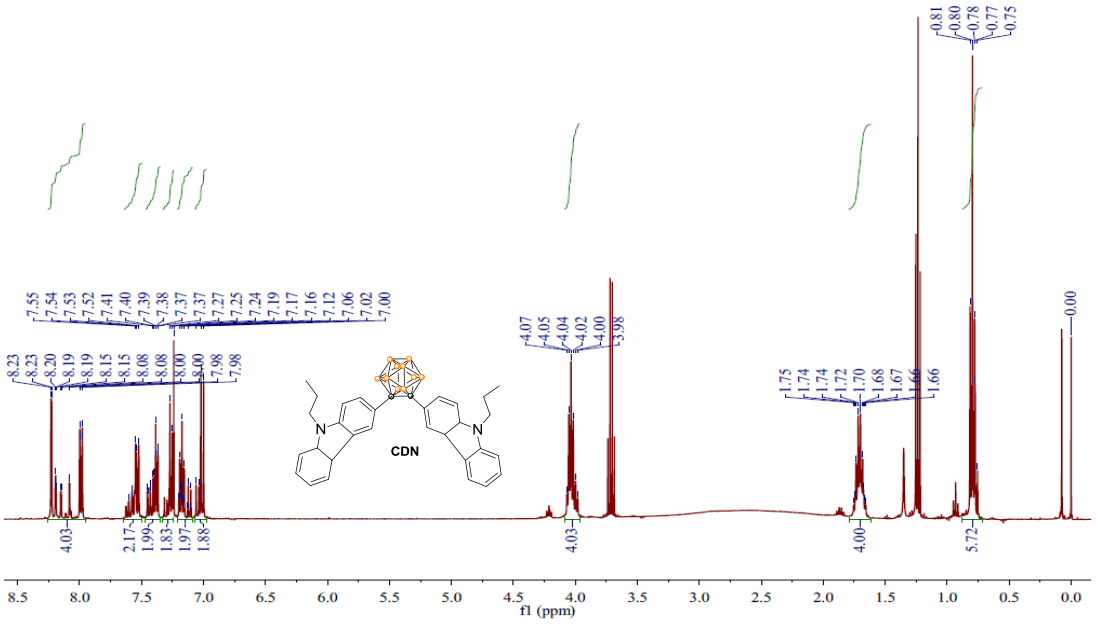

Figure S19. ^{1}H NMR spectroscopies of **CDN** in $CDCl_3$.

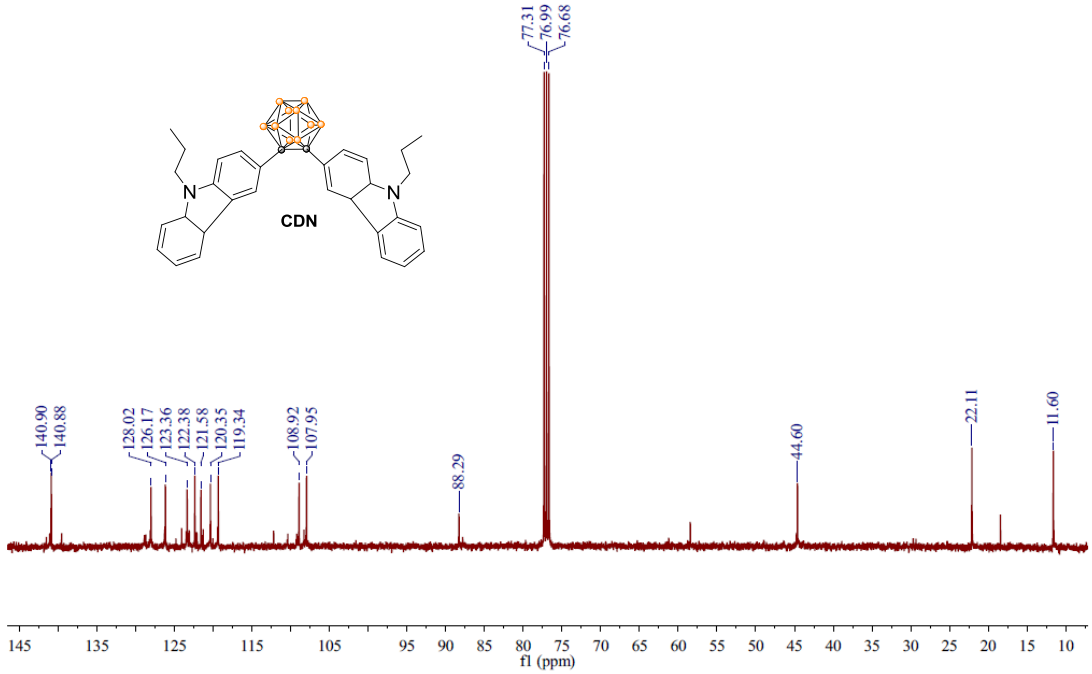

Figure S20. ^{13}C NMR spectroscopies of **CDN** in $CDCl_3$.

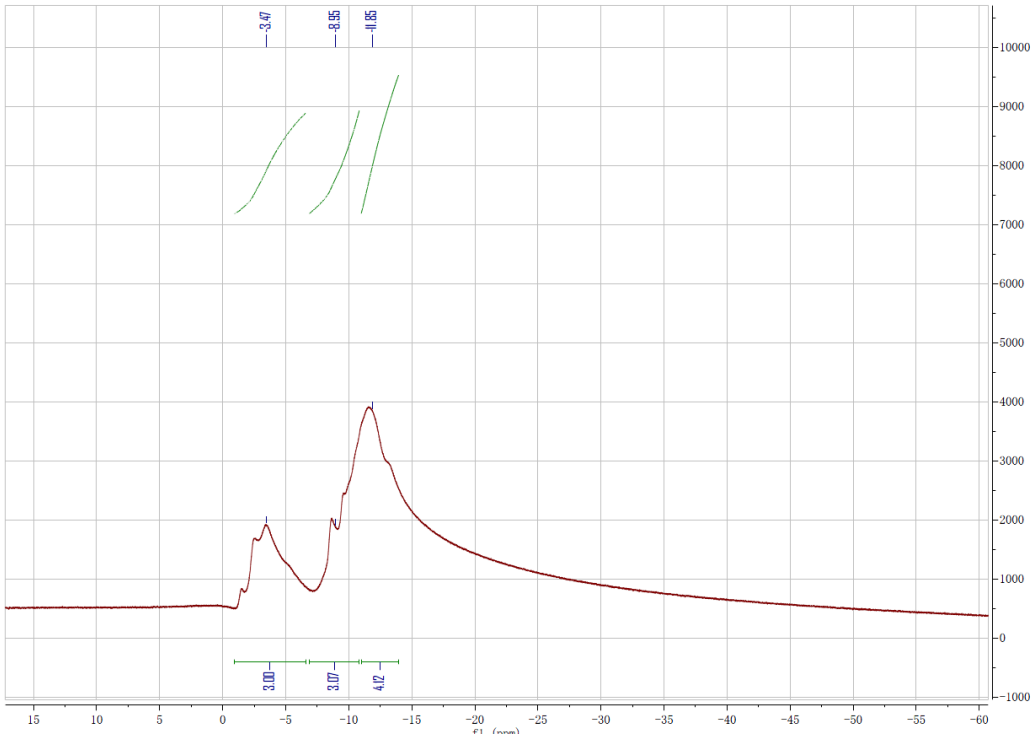

Figure S21. ^{11}B NMR spectroscopies of **CDN** in $CDCl_3$.

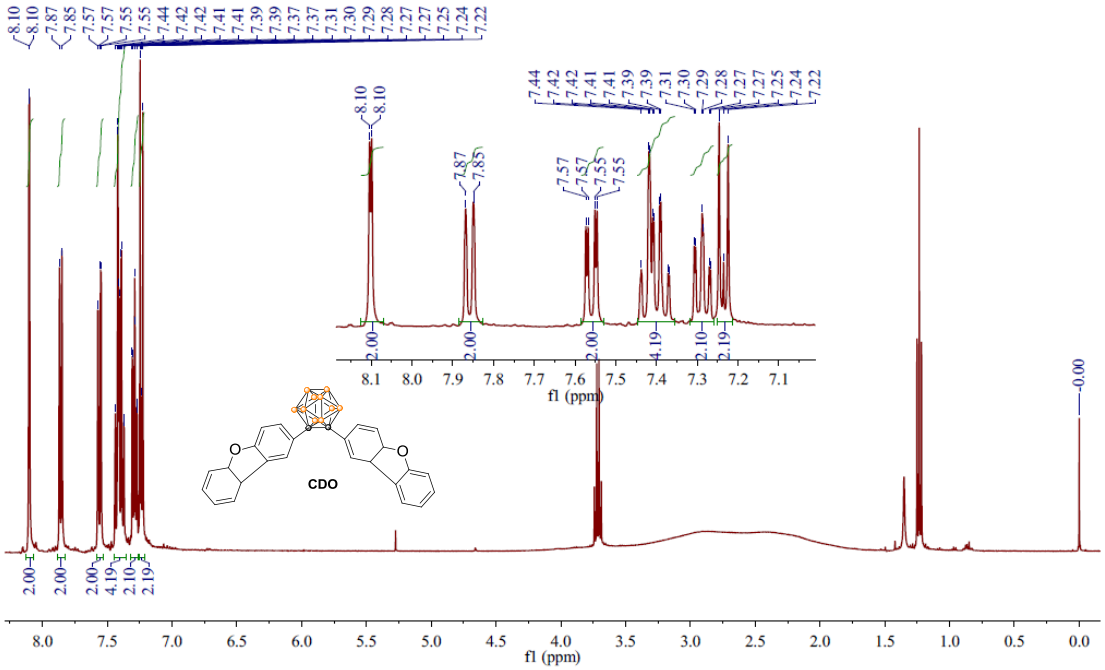

Figure S22. ^{1}H NMR spectroscopies of **CDO** in $CDCl_3$.

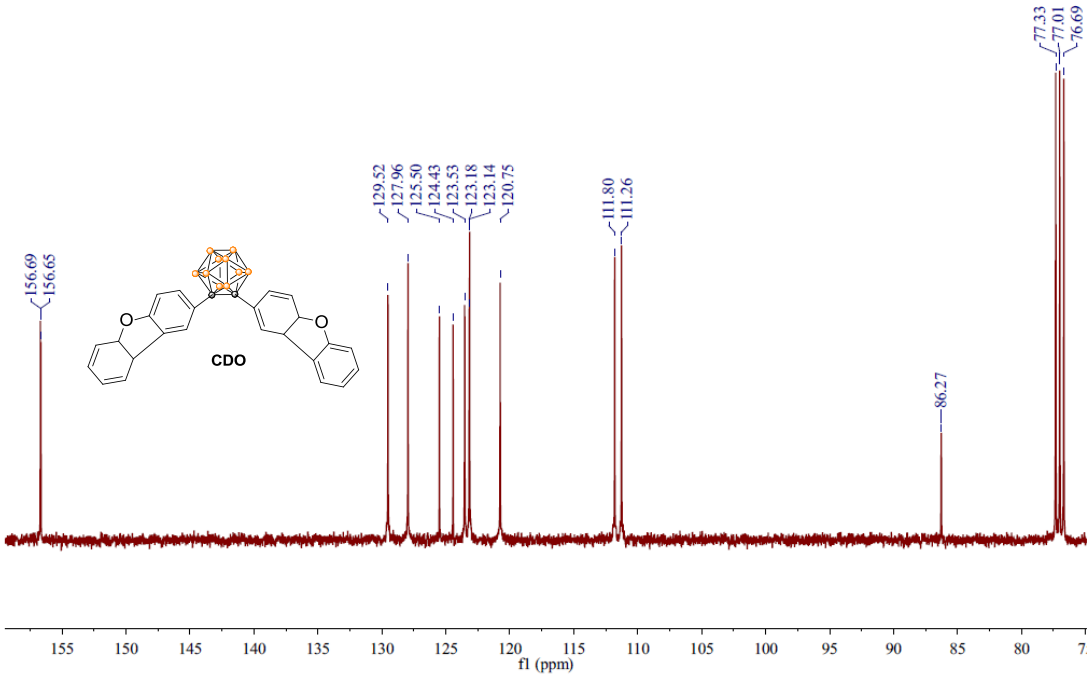

Figure S23. ^{13}C NMR spectroscopies of **CDO** in $CDCl_3$.

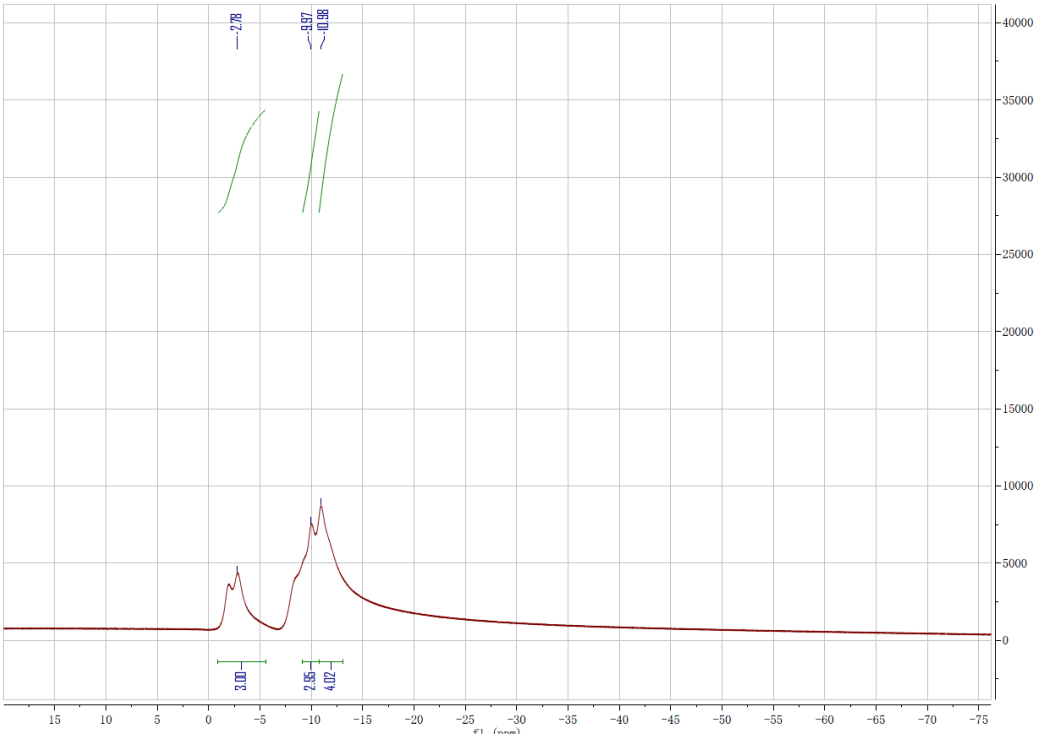

Figure S24. ^{11}B NMR spectroscopies of **CDO** in $CDCl_3$.

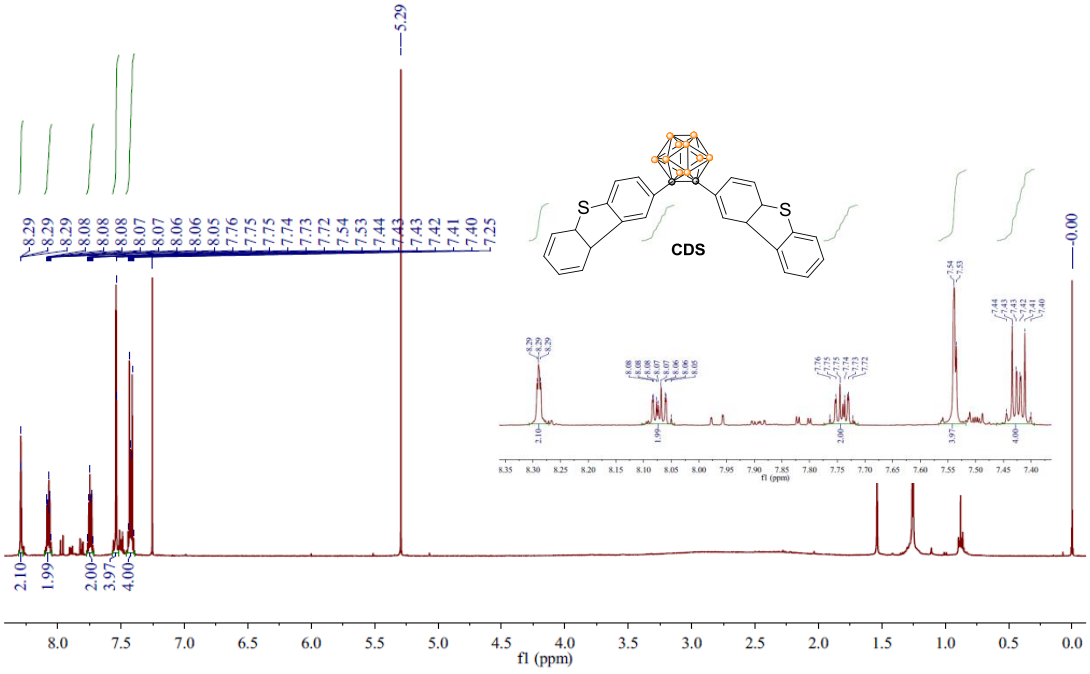

Figure S25. ^{1}H NMR spectroscopies of **CDS** in $CDCl_3$.

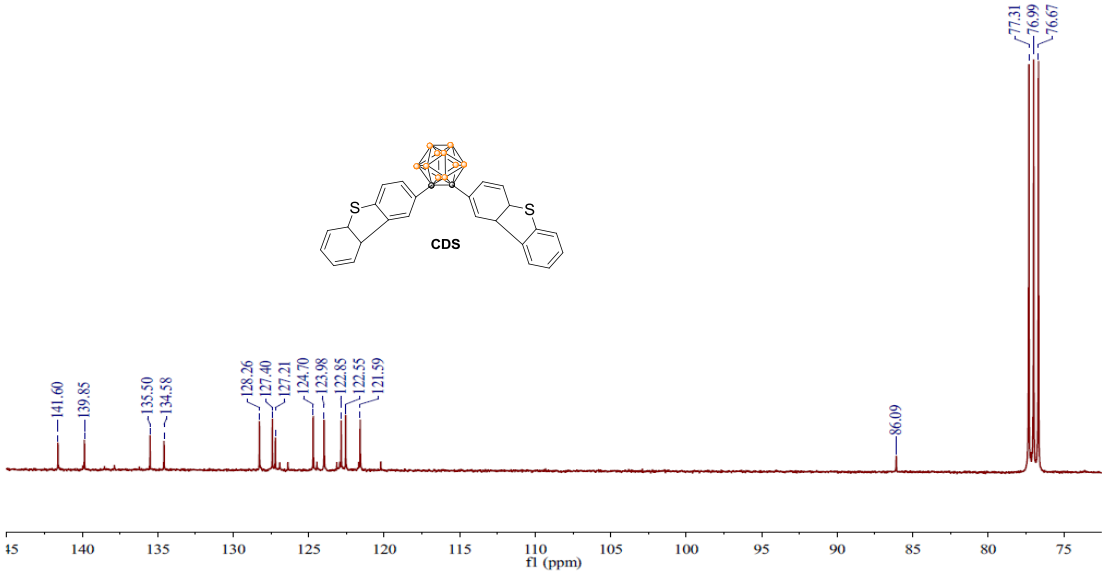

Figure S26. ^{13}C NMR spectroscopies of **CDS** in $CDCl_3$.

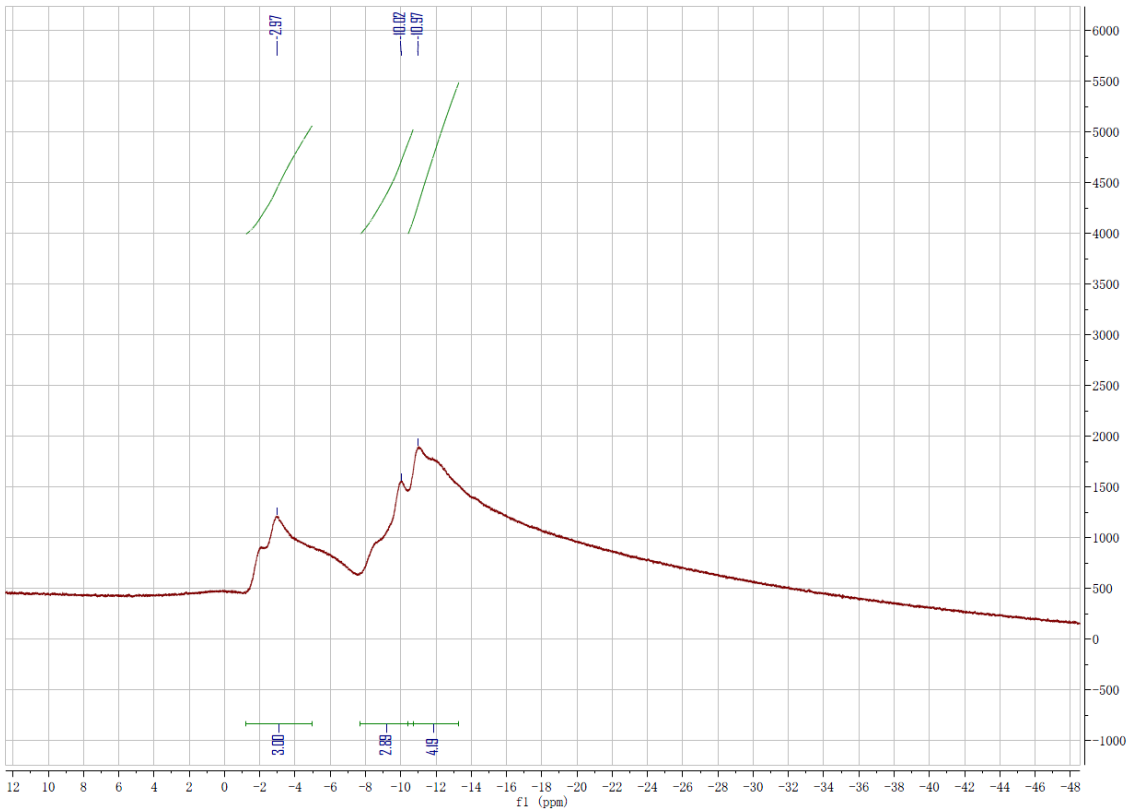

Figure S27. ^{11}B NMR spectroscopies of **CDS** in $CDCl_3$.